ELSEVIER

Polymer 42 (2001) 7781–7789

polymer

www.elsevier.nl/locate/polymer

Gas sorption and transport in poly(alkyl (meth)acrylate)s. II. Sorption and diffusion properties

Z. Mogri, D.R. Paul*

Department of Chemical Engineering, Texas Materials Institute, The University of Texas at Austin, CPE 3.454, Austin, TX 78712-1062, USA

Received 12 December 2000; received in revised form 30 March 2001; accepted 2 April 2001

Abstract

Gas sorption in amorphous ethyl and decyl acrylate polymers and semi-crystalline and molten octadecyl and behenyl acrylate polymers were measured as a function of temperature for CH_4 and CO_2. Diffusion coefficients, calculated based on permeability data for these polymers, are found to increase with increasing side-chain length. The large differences in permeability observed between poly(methyl acrylate) and poly(ethyl acrylate) are described in terms of the diffusion and solubility of gases in these polymers. Anomalous permeation switch behavior of poly(behenyl acrylate) is further analyzed using diffusion switch data. The solubility coefficients for CH_4 and CO_2 in amorphous poly(alkyl acrylate)s are correlated with alkyl content and extrapolated to the long side-chain limit. The extrapolated values are larger than those for amorphous polyethylene found by extrapolation to zero crystallinity using the traditional two-phase model.

Keywords: Side-chain crystalline polymers; Alkyl acrylates; Sorption switch

1. Introduction

Gas sorption in main-chain semi-crystalline polymers is generally described by a two-phase model that views crystallites as non-sorbing with no influence on the amorphous phase. The Michaels and Bixler model [1–3] for the gas solubility coefficient, S, is given by

$$S = S^* \alpha \tag{1}$$

where S^* is the solubility coefficient of the completely amorphous polymer and α the amorphous volume fraction. Originally developed to fit solubility data in rubbery polyethylene, this model appears to describe several other systems including glassy poly(ethylene terephthalate) [4,5]. In these prior studies, the value of S^* was found by extrapolation of data on samples of varying crystallinity. To our knowledge, only one study has confirmed the above model using a series of materials that included the completely amorphous polymer [6]. Furthermore, other studies have shown that penetrants may sorb in the crystalline regions of some polymers [7–9].

The question of whether or not the crystallites affect the nature of the amorphous phase, with regard to solubility, and if this amorphous phase can be treated as a liquid, as in the above model, must be addressed. Budzien et al. [10] estimated the gas solubility in amorphous polyethylene by an extrapolation of gas solubility in alkanes and found a value approximately twice that of the extrapolation performed by Michaels and Bixler. Clearly, there is no sharp delineation between the crystalline and amorphous regions [11] and there is clear evidence that the crystallites have a great influence on the mobility in the surrounding amorphous phase. Solid-state NMR measurements of several main-chain crystalline polymers reveal an interfacial amorphous phase of substantially less mobility than the bulk amorphous phase. The T_2 relaxation time for the interface of polycaprolactone was shown to be 64 times slower than the bulk amorphous phase [12]. Similar order of magnitude differences were noted for polyethylene and hydrogenated polybutadiene [13,14]. In fact, the model proposed by Michaels and Bixler [3] for diffusion in semi-crystalline polymers partially takes this stiffened amorphous phase into account:

$$D = D^*/\tau\beta \tag{2}$$

where D^* is the diffusion coefficient of the completely amorphous polymer, τ the tortuosity and β a chain immobilization factor accounting for the reduced penetrant mobility in the amorphous phase surrounding the crystallites.

Part 1 described gas permeation behavior in side-chain

* Corresponding author. Tel.: +1-512-471-5392; fax: +1-512-471-0542.
E-mail address: drp@che.utexas.edu (D.R. Paul).

0032-3861/01/$ - see front matter
PII: S0032-3861(01)00261-0

crystalline poly(alkyl acrylate)s above and below the melting point [15]. The change in permeation on traversing the melting point was significantly greater for these materials than observed for polycaprolactone in both magnitude and penetrant dependence. These trends were attributed to differences in crystalline morphology and a larger chain immobilization effect by the crystallites on the amorphous phase of the side-chain crystalline alkyl acrylates. This paper examines gas sorption in these materials. The sorption data reported here allows factoring the permeation effects described in Part 1 into their solubility and diffusivity components. Gas sorption data is only reported for CH_4 and CO_2 owing to the accuracy of measurement for these gases compared to the other penetrants reported here and to keep the scope of this study manageable.

2. Experimental

The polymerization, characterization and permeability measurement techniques used were documented in the previous paper [15]. Equilibrium gas sorption isotherms were measured with a dual volume, pressure decay apparatus described elsewhere [16]. This apparatus was immersed in a thermostated water bath. Due to its tackiness, poly(ethyl acrylate) (PA-2) film was placed on aluminum foil and rolled into a cylindrical shape before loading into the apparatus. The volume of the aluminum was subtracted from the dead volume of the cell when calculating the solubility coefficient. Amorphous poly(decyl acrylate) (PA-10) and molten poly(behenyl acrylate) (PA-22) were tested without the use of aluminum foil. It was confirmed that the polymer forms a molten pool in the bottom of the dead volume as a fluid. Yet, equilibrium was routinely reached within 24 h. While performing solubility measurements in the molten state, poly(octadecyl acrylate) (PA-18) and PA-22 were degassed in molten form in a vacuum oven before the temperature was incremented.

3. Results and discussion

The solubility and diffusivity data for amorphous poly(alkyl acrylate)s are first documented; the diffusion coefficients were calculated from $D = P/S$. The large change in permeability going from poly(methyl acrylate)

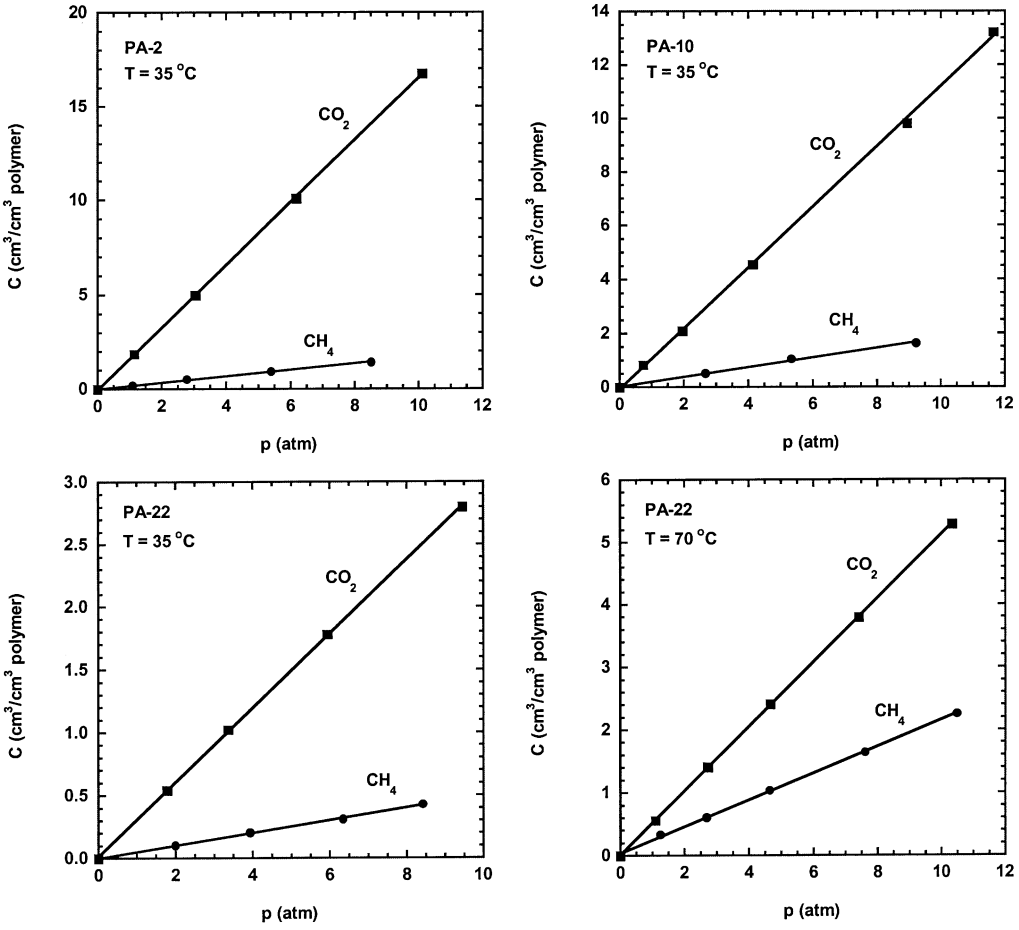

Fig. 1. Representative CH_4 and CO_2 sorption isotherms for PA-2, PA-10 at 35°C and PA-22 in the semi-crystalline state (cooled at 1°C/min) at 35°C and molten state at 70°C. The solubility follows Henry's law at the pressures and temperatures studied.

(PA-1) to PA-2 described in Part 1 is analyzed here using the solubility and diffusion coefficients for these polymers. An asymptotic limit for the diffusion coefficient at very long side-chain lengths is also discussed. The lower permeability switch of PA-22 compared to PA-18 is also explained in terms of the solubility and diffusivity switch for both polymers. Finally, the solubility in the amorphous state is revisited and described as a function of the alkyl composition in the polymer. Some apparent inconsistencies in the two-phase model for describing solubility in semi-crystalline polymers are indicated.

3.1. Solubility and diffusivity in the amorphous state of poly(alkyl acrylate)s

Representative CH_4 and CO_2 sorption isotherms for rubbery and amorphous PA-2 and PA-10 at 35°C and semi-crystalline and molten PA-22 at 35 and 70°C are shown in Fig. 1. Henry's law is obeyed in every case. The solubility of CH_4 and CO_2 was measured as a function of temperature for all polymers and was found to follow typical van't Hoff behavior in both the semi-crystalline and molten states.

Table 1
CH_4 and CO_2 permeability (P), solubility (S) and diffusion (D) coefficients and activation energies of permeation (E_p) and diffusion (E_d) and heats of sorption (ΔH_s) of poly(alkyl acrylate)s of varying side-chain length in the amorphous or molten state

Gas	n	P[a]	S[b]	D[c] $\times 10^{-6}$	E_p[d]	ΔH_s[d]	E_d[d]
CH_4	1	0.29	0.15[e]	0.0148	–	–	–
	2	14.9	0.17	0.664	8.1	−2.4	10.5
	10	47.8	0.18	1.98	6.8	−1.9	8.7
	18	90.8	0.21	3.23	5.6	−1.6	7.2
	22	93.0	0.24	2.92	4.9	−0.8	5.7
CO_2	1	9.58	1.98[e]	0.0368	–	–	–
	2	176	1.67	0.801	5.0	−3.4	8.4
	10	261	1.12	1.77	4.2	−2.9	7.1
	18	428	1.26	2.58	2.7	−6	8.7
	22	404	0.71	4.35	2.9	−1.9	4.8

[a] P measured at or extrapolated to 35°C and has units of Barrers.
[b] S measured at or extrapolated to 35°C and has units of cm^3/cm^3 polymer atm.
[c] Calculated from $D = P/S$ at 35°C with units of cm^2/s.
[d] E_p, ΔH_s and E_d have units of kcal/mol.
[e] From Ref. [18].

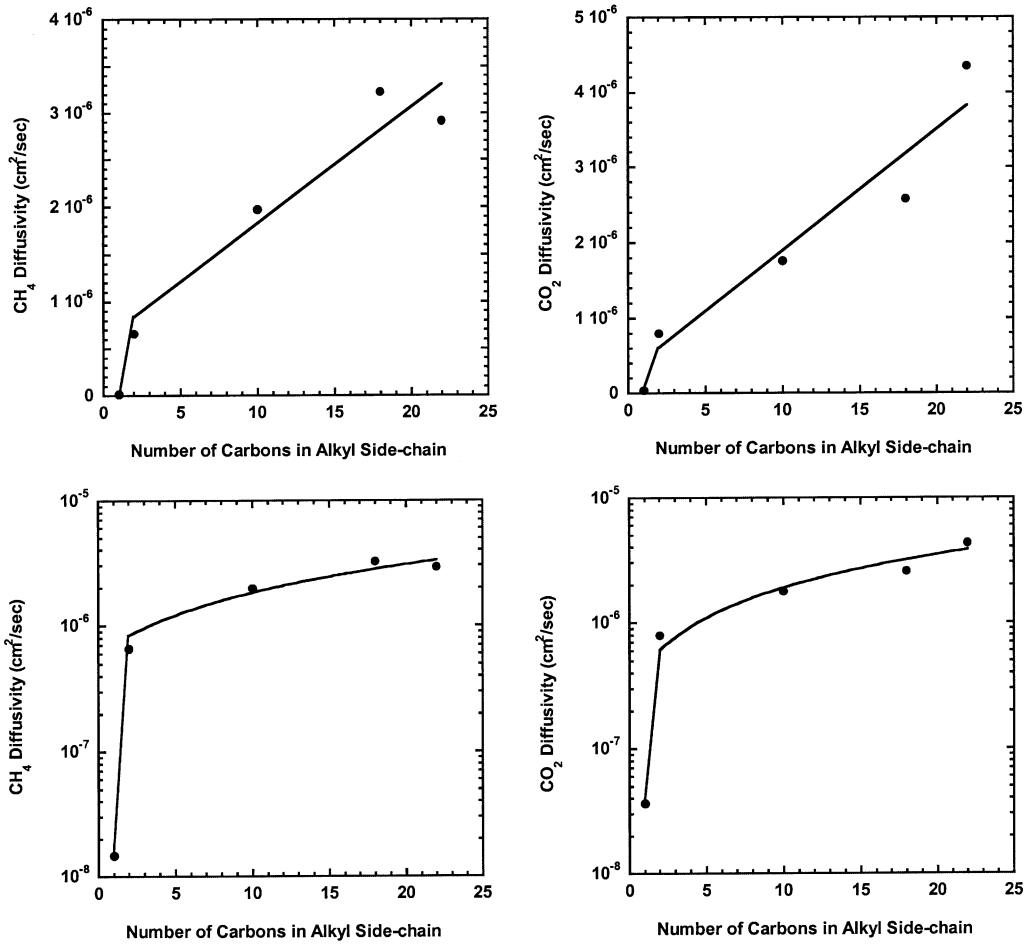

Fig. 2. CH_4 and CO_2 diffusion coefficients (cm^2/s) (on arithmetic and logarithmic scales) of amorphous poly(alkyl acrylate)s as a function of side-chain length at 35°C.

Table 2
CH_4 and CO_2 permeability, solubility and diffusion coefficients for glassy poly(alkyl methacrylate)s and rubbery poly(alkyl acrylate)s illustrating the source of 'jump' in permeability upon addition of the first methylene group in these series

Polymer	CH_4			CO_2		
	P[a]	S[b]	D[c]	P[a]	S[b]	D[c]
PMA-1[d]	0.0058	0.39	1.14×10^{-10}	0.36	3.44	7.90×10^{-10}
PMA-2[e]	0.347	0.16	1.60×10^{-8}	7.01	1.48	3.59×10^{-8}
PMA-2/PMA-1	59.8	0.41	141	19.5	0.43	45.4
PA-1	0.29	0.15[f]	1.48×10^{-8}	9.58	1.98[f]	3.68×10^{-8}
PA-2	14.9	0.17	6.64×10^{-7}	176	1.67	8.01×10^{-7}
PA-2/PA-1	51.7	1.17	44.8	18.3	0.84	21.8

[a] P given at 35°C and has units of Barrers.
[b] S given at 35°C and has units of cm^3/cm^3 polymer atm.
[c] D given at 35°C and has units of cm^2/s.
[d] From Refs. [25,26].
[e] From Refs. [26,27].
[f] From Refs. [18,26].

The amorphous state gas transport coefficients listed in Table 1 include previously reported data for PA-18 [17]. The increase in permeability with side-chain length reported in the previous paper [15] primarily reflects trends in the diffusion coefficient as shown in Fig. 2 for CH_4 and CO_2. The diffusion coefficients for PA-1 were calculated from the permeability data of Part 1 and solubility data determined earlier in our laboratory [18]. As shown earlier for the permeability coefficient [15], there is a dramatic increase in the diffusivity from PA-1 to PA-2 and a fairly linear increase thereafter, though there is some scatter in the data. It is useful to present this data on a logarithmic scale shown also in Fig. 2.

The large difference in permeability between PA-1 and PA-2 is examined in terms of the solubility and diffusion contributions in Table 2 for CH_4 and CO_2. The glassy methyl and ethyl methacrylate polymers (PMA-1 and -2) have lower diffusivities than the corresponding rubbery acrylate polymers (PA-1 and -2), as might be expected. There is a large increase in the diffusivity for both sets of polymers upon addition of the extra methylene unit; however, the increase is greater for the glassy polymers. The extra methylene significantly decreases the solubility coefficient for glassy polymethacrylates; however, for the rubbery polyacrylates, this leads to a small increase for CH_4 and a small decrease for CO_2. Solubility contributes about a factor of two or more to the permeability increase caused by the extra methylene for the rubbery materials than the glassy ones. Though CO_2 has a larger diffusivity than CH_4 for each set of polymers, it is the change in diffusivity that gives rise to the size dependence, possibly due to a more flexible backbone and higher free volume.

Table 3
CO_2 diffusivity (D) and solubility (S) and activation energies of diffusion (E_d) and heats of sorption (ΔH_s) in amorphous polyethylene and amorphous analogs of polyethylene

Polymer	T (°C)	$D^a\times10^{-6}$	E_d[b]	$D\times10^{-6}$ (35°C)	S[c]	ΔH_s[b]	S (50°C)	Reference
PA-22	35	4.35	4.8	4.35	0.71	−1.9	0.61	This work
Natural rubber	25	1.24	8.2	1.95	0.94	−3.0	0.64	[3]
Natural rubber	25	1.10	8.9	1.79	0.90	−2.8	0.63	[28]
Methyl rubber	25	0.063	12.8	0.127	0.90	−1.6	0.73	[28]
Butyl rubber	25	0.0578	12.0	0.112	0.68	−2.1	0.52	[28]
Polymethylpentadiene	50	0.438	8.3	0.233	1.10	–	1.10	[28]
Molten gutta percha	50	4.13	9.2	2.05	0.69	−2.5	0.69	[28]
Polybutadiene	50	2.78	7.3	1.60	0.72	−2.1	0.72	[28]
Molten polybutadiene (48% *trans*)	25	0.206	6.4	0.292	0.96	−3.0	0.65	[29]
Molten polyethylene	188	56.9	4.4	5.21	0.24	−0.8	0.34	[30,31]
Polyethylene ($\alpha\rightarrow1$)	25	–	–	–	0.45	−2.8[d]	0.31	[2]
Amorphous polyethylene	25	–	–	–	0.99	−2.8[d]	0.68	[10]
Molten polypropylene	188	42.4	3.0	8.32	0.20	−1.7	0.43	[30,31]

[a] Calculated from $D = P/S$ at 35°C with units of cm^2/s.
[b] E_d and ΔH_s have units of kcal/mol.
[c] S has units of cm^3/cm^3 polymer atm.
[d] Natural rubber ΔH_s from Ref. [28].

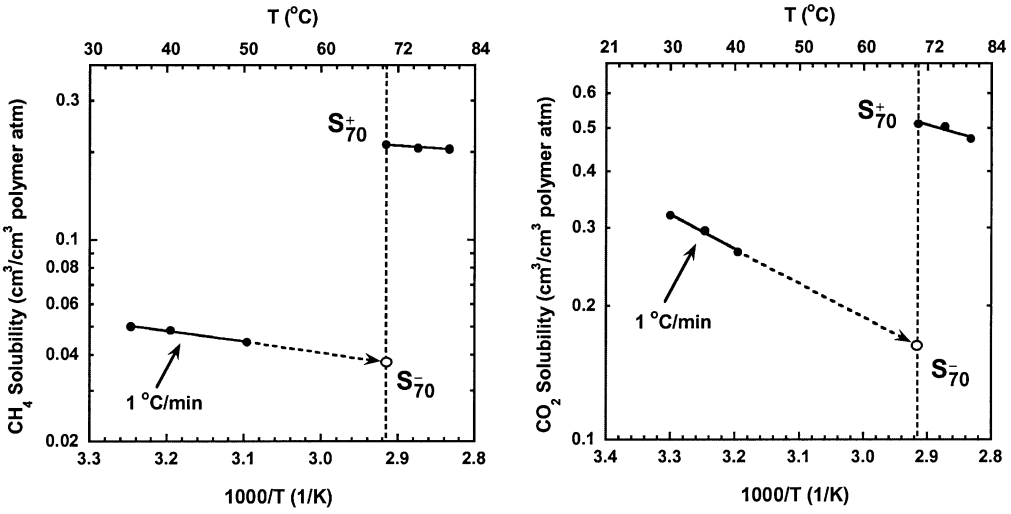

Fig. 3. CH_4 and CO_2 solubility coefficients for PA-22 as a function of temperature. The semi-crystalline state measurements were made with polymer cooled from the melt at 1°C/min. The solubility switch is calculated from the extrapolated values of the semi-crystalline and molten states (S_{70}^{+} and S_{70}^{-}).

As described earlier for permeability, at very long side-chain lengths, one might expect the diffusion coefficient of amorphous polyacrylates to approach that of amorphous polyethylene. The arithmetic plots do not indicate an asymptotic limit; however, the logarithmic plots shown in Fig. 2 suggest that such an asymptote may exist. The diffusion behavior in amorphous polyethylene has not been studied extensively; nevertheless, the limited data for amorphous polyethylene and for some polymers of similar structure are compiled in Table 3 for CO_2. When compared at the common temperature of 35°C by appropriate extrapolation, the diffusion coefficients for most of these polymers are well below that of PA-22. However, both molten polyethylene and polypropylene have higher values, when extrapolated to 35°C, which is consistent with the hypothesis of an asymptotic limit for the diffusion coefficient of these side-chain acrylates. A similar comparison for CH_4 is not possible since, to our knowledge, such data are not available for any of these polymers except for natural rubber whose value is a factor of two lower than that for PA-22. Clearly, further data are needed to unambiguously evaluate this hypothesis.

The results in Table 1 also show that as the alkyl unit becomes longer, the activation energy of diffusion decreases, following the same trend as E_p [15], while the heat of sorption generally becomes more endothermic.

3.2. Solubility and diffusivity switch for poly(behenyl acrylate)

The solubility and diffusivity switch values are calculated in the same way as described previously for permeability.

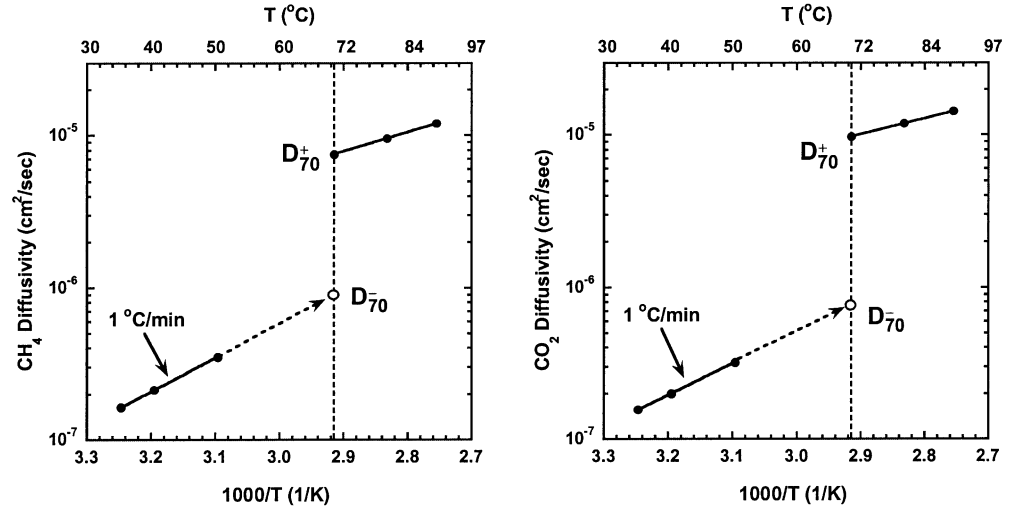

Fig. 4. CH_4 and CO_2 diffusivity coefficients for PA-22 as a function of temperature. The semi-crystalline state measurements were made with polymer cooled from the melt at 1°C/min. The diffusivity switch is calculated from the extrapolated values of the semi-crystalline and molten states (D_{70}^{+} and D_{70}^{-}).

Table 4
Comparison of thermal switch values for permeability, solubility and diffusivity of PA-18 and PA-22. T is the temperature of the switch, 50°C for PA-18 and 70°C for PA-22 (note that the ratio of solubility coefficients shown here are the inverse of the convention used for the permeability and diffusion coefficients in order to facilitate comparison of the solubility ratio to α as predicted by Eq. (3))

Polymer	α	CH_4			CO_2		
		P_T^+/P_T^-	S_T^-/S_T^+	$D_T^+/D_T^- = \tau\beta$	P_T^+/P_T^-	S_T^-/S_T^+	$D_T^+/D_T^- = \tau\beta$
PA-18	0.63	81.5	0.31	25.2	61.1	0.37	22.5
PA-22	0.53	48.1	0.18	8.7	40.1	0.31	12.8

That is, the solubility and diffusivity data in the semi-crystalline and molten states are extrapolated to the polymer melting temperature as shown in Figs. 3 and 4. The ratio of these extrapolated values characterize the switch on melting. According to the models proposed in Eqs. (1) and (2), the solubility and diffusivity switch values should be given by

$$\frac{S_T^-}{S_T^+} = \alpha \tag{3}$$

$$\frac{D_T^+}{D_T^-} = \tau\beta \tag{4}$$

where the superscript $(-)$ indicates values in the semi-crystalline state, the superscript $(+)$ indicates values in the molten state and T the temperature where the comparison is made, usually T_m. The corresponding P, D and S ratios are shown in Table 4 for CH_4 and CO_2 in PA-18 and PA-22. The semi-crystalline state for both polymers was established by cooling from the melt at 1°C/min. Note that the solubility switch ratio is constructed here using the inverse of the convention used for the permeability and diffusivity ratios to permit comparisons with α expected by Eq. (3).

The solubility ratios for both PA-18 and PA-22 are less than the value of α determined calorimetrically by approximately a factor of 2. Thus, it is quite clear that $S_T^-/S_T^+ \neq \alpha$ for these side-chain crystalline polymers. Note that the value of the solubility ratio also depends on the penetrant which is contrary to the simple model expressed by Eq. (3). Of course, as noted previously [15], there is a change in composition on melting, and an attempt to account for this is made in the next section. The solubility change on melting is larger for PA-22 than PA-18 for both penetrants and accounts for a factor of 3–5 of the permeation jump.

The diffusion switch plays a larger role in the permeation jump and is dependent on size, as may be expected. The lower permeation jump for PA-22 compared to PA-18 is largely due to the lower diffusion jump for the former. This could well be due to different morphologies in the semi-crystalline state including crystallite size and shape. As seen in Table 5, there is a much higher diffusion coefficient in the semi-crystalline state for PA-22 than PA-18. One cannot quantitatively test the validity of Eq. (4) since a priori determinations of either τ and β are not presently possible. In fact, Michaels [19] noted the complexities of estimating the tortuosity of two-phase materials without complete knowledge of their geometry.

As stated in Part 1, there is a clear decrease in activation energy of permeation upon traversing the melting point, indicative of chain immobilization effects, as has been documented for main-chain crystalline polymers [20,21]. It is of interest to note the contributions from diffusion and solubility to this decrease. One might expect most of the difference to be accounted for in the diffusion activation energy since the chain immobilization term appears in Eq. (4). A comparison of Tables 1 and 5 shows substantially lower activation energies of diffusion in the molten state compared to the semi-crystalline state and generally accounts for most of the difference in E_p above and below the melting point. But also note the generally lower heats of sorption in the molten state compared to the semi-crystalline state. This behavior is not supported by Eq. (3) and is further evidence that a simple two-phase model does not describe these systems and chain immobilization may affect the solubility of gases in side-chain crystalline materials. The difference in the heat of sorption in the molten and semi-crystalline states also contributes to the difference in E_p but generally to a lesser degree than the difference in E_d.

3.3. Effect of alkyl composition on solubility in the amorphous state of poly(alkyl acrylate)s

As seen in Table 1, the solubility coefficients for gases in poly(alkyl acrylate)s above T_m depend on the length of the

Table 5
CH_4 and CO_2 permeability (P), solubility (S) and diffusion (D) coefficients of PA-18 and PA-22 in the semi-crystalline state (established by cooling from the melt at 1°C/min). T is the temperature of the switch, 50°C for PA-18 and 70°C for PA-22

Gas	n	α	P_T^- [a]	S_T^- [b]	$D_T^- \times 10^{-6}$ [c]	E_p [d]	ΔH_s [d]	E_d [d]
CH_4	18	0.63	1.70	0.06	0.221	13.1	−2.6	15.7
	22	0.53	4.37	0.04	0.873	8.3	−1.7	10.0
CO_2	18	0.63	8.58	0.30	0.221	9.2	−2.3	11.5
	22	0.53	16.2	0.16	0.757	5.9	−3.5	9.4

[a] P has units of Barrers.
[b] S has units of cm^3/cm^3 polymer atm.
[c] Calculated from $D = P/S$ with units of cm^2/s.
[d] E_p, ΔH_s and E_d have units of kcal/mol.

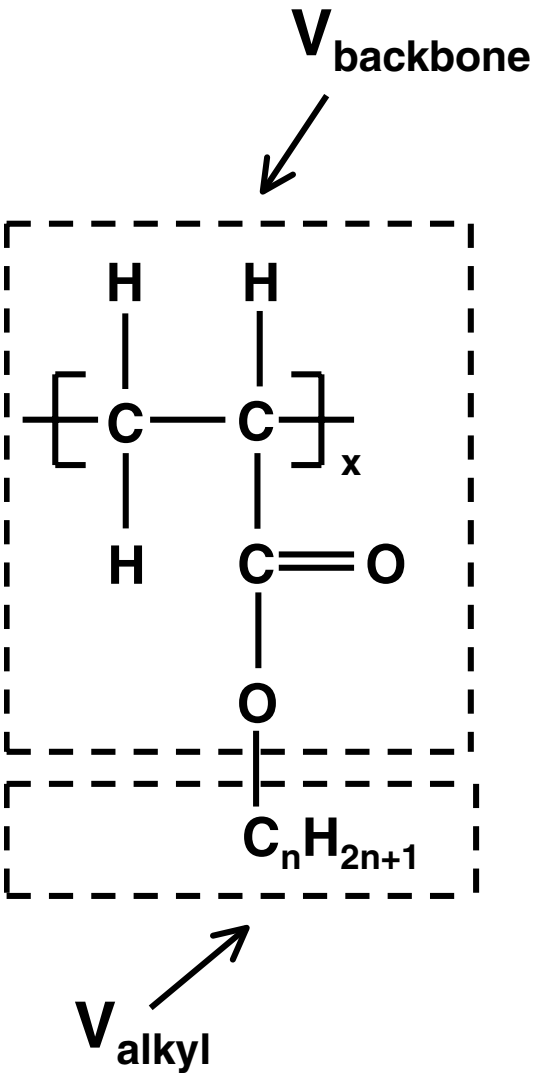

Fig. 5. Structure of poly(alkyl acrylate) illustrating the backbone and alkyl units comprising the polymer. The van der Waals volumes were computed for these units and the alkyl volume fraction was calculated. These values are shown in Figs. 6 and 7.

alkyl side-chain. As suggested previously [15] for the gas transport properties of molten alkyl acrylate polymers, one might expect gas solubility coefficients to approach the values for amorphous polyethylene in the limit of very long side-chains. An appropriate way to explore this proposal is to plot the gas solubility coefficients of poly(alkyl acrylate)s as a function of the volume fraction of alkyl units in these materials. The alkyl volume fraction was calculated from

$$\Phi = \frac{V_{\text{alkyl}}}{V_{\text{alkyl}} + V_{\text{backbone}}} \tag{5}$$

where V_{alkyl} and V_{backbone} are the van der Waals volumes, computed by group contribution methods [22] for each of the two portions of the repeat units shown in Fig. 5.

Figs. 6 and 7 show the CH_4 and CO_2 solubility coefficients

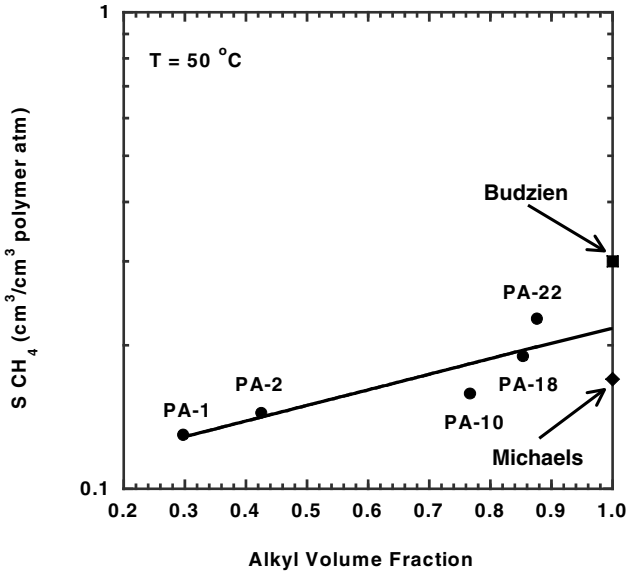

Fig. 6. Dependence of CH_4 solubility on the composition of alkyl units in amorphous and molten polymers measured at or extrapolated to 50°C. The solubility for PA-1 was calculated from data in Ref. [18] using the heat of sorption from Table 6.

plotted on a log scale as a function of the alkyl volume fraction; the form suggested by theoretical arguments for homogeneous multicomponent polymers or copolymers [23]. The extrapolation error from the values given at 35°C in Table 1 to 50°C seen in Figs. 6 and 7 is less than 7% for the acrylate polymers except for PA-1. The solubility coefficients for PA-1 at 50°C were estimated from values at 35°C [18] using a heat of sorption of −1.3 kcal/mol for CH_4 and −2.3 kcal/mol for CO_2, which are taken as typical values, see Tables 3 and 6; this temperature correction is

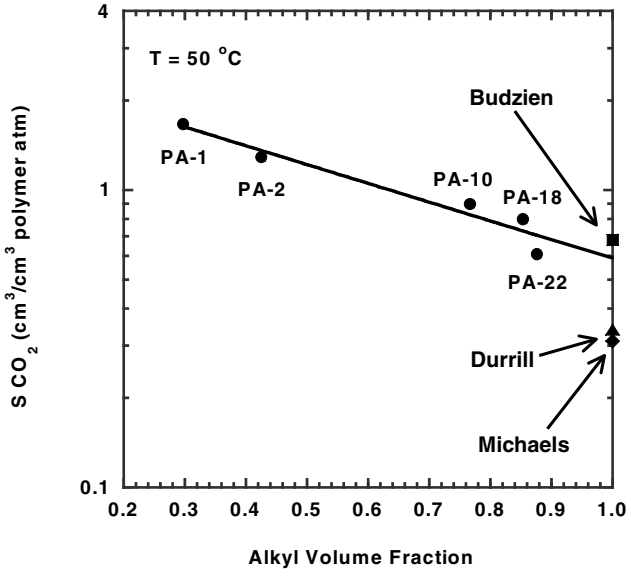

Fig. 7. Dependence of CO_2 solubility on the composition of alkyl units in amorphous and molten polymers measured at or extrapolated to 50°C. The solubility for PA-1 was calculated from data in Ref. [18] using the heat of sorption averaged from the values in Table 3.

relatively small in any case. The plots shown in Figs. 6 and 7 form a reasonable correlation of the data for the various poly(alkyl acrylate)s, and the line drawn is the best linear fit. The extrapolation of this line to an alkyl volume fraction of unity will be compared below to other estimates for amorphous polyethylene.

CH_4 solubility increases while CO_2 solubility decreases with increasing alkyl volume fraction. Qualitatively, these trends make sense. Increasing the hydrocarbon content should lead to a more favorable thermodynamic interaction with CH_4. On the other hand, diluting the polarity of the acrylate polymers by longer alkyl units should lead to less favorable interactions with CO_2. An earlier study noted an increase in the CO_2/CH_4 solubility ratio as the polarity increased in low molecular weight solvents and other various polymers [24]; this is entirely consistent with the trends in Figs. 6 and 7.

The extrapolation of the lines shown in Figs. 6 and 7 to an alkyl volume fraction of unity falls well above the predictions of CH_4 and CO_2 solubility in amorphous polyethylene proposed by Michaels and Bixler. While there is some scatter in the data for CH_4, the extrapolation yields a value of 0.22 cm^3/cm^3 polymer atm which is close to the value for natural rubber (see Table 6) but in between the values predicted for amorphous polyethylene by Budzien et al. and Michaels and Bixler (see Fig. 6). The plot for CO_2 has less scatter and the extrapolation yields a value of 0.59 cm^3/cm^3 polymer atm, which again is close to that of natural rubber (see Table 3) and is much closer to the estimate for amorphous polyethylene reported by Budzien et al. than those reported by Michaels and Bixler or by Durrill and Griskey (see Table 3 and Fig. 7).

The effect that the compositional change on melting has on the value of the solubility switch ratio for PA-18 can now be evaluated. PA-10 has the same number of carbons in the amorphous state as does semi-crystalline PA-18; hence, the S_T^+ values of 0.16 cm^3/cm^3 polymer atm for CH_4 and 0.91 cm^3/cm^3 polymer atm for CO_2 are substituted for those of PA-18 at $T = 50$°C. The S_T^- values of PA-18 remain the same for this calculation. The corrected solubility switch value (S_T^-/S_T^+) increases from 0.31 to 0.38 for CH_4 but decreases from 0.37 to 0.33 for CO_2. The corrected values are still well below the value of α determined from the heat of fusion indicating that accounting for the compositional change does not reconcile the discrepancy between S_T^-/S_T^+ and α predicted by the simple model of Michaels and Bixler.

Table 6
CH_4 solubility in amorphous polyethylene and amorphous analogs of polyethylene. Solubility and ΔH_s have units of cm^3/cm^3 polymer atm and kcal/mol

Polymer	T (°C)	S	ΔH_s	S at 50°C	Reference
Natural rubber	25	0.25	− 1.3	0.21	[3]
Polyethylene ($\alpha = 1$)	25	0.20	− 1.3[a]	0.17	[3]
Amorphous polyethylene	25	0.36	− 1.3[a]	0.30	[10]

[a] Natural rubber ΔH_s from Ref. [3].

4. Conclusions

Data for the solubility of CH_4 and CO_2 in amorphous and semi-crystalline poly(alkyl acrylate)s have permitted further analysis of permeation trends presented earlier [15]. The increase in permeability as the side-chain length increases and the large change in permeability in going from PA-1 to PA-2 are predominantly due to trends in the diffusion coefficient and not solubility. The semi-crystalline state diffusion coefficient for PA-22 is significantly higher than for PA-18 and is a major factor in the lower permeability switch of PA-22 despite a higher degree of crystallinity. Gas solubility in amorphous acrylates was found to depend on the alkyl composition of the polymer. An extrapolation of the solubility data to an alkyl volume fraction of unity was compared to that of amorphous polyethylene. This method of estimating the solubility in amorphous polyethylene leads to substantially higher values than found by extrapolation of semi-crystalline polyethylene data to the amorphous state. This combined with an analysis of the change in solubility on melting of the side-chain crystalline poly(alkyl acrylate)s suggests that the simple two-phase model of Michaels and Bixler may not fully describe the effect of crystallinity on solubility.

Acknowledgements

This research was funded by National Science Foundation grant number CTS 97-14305 administered by the Division of Chemical and Transport Systems — Separation and Purification Processes Program.

References

[1] Michaels AS, Parker RB. J Polym Sci 1959;41:53–71.
[2] Michaels AS, Bixler HJ. J Polym Sci 1961;50:393–412.
[3] Michaels AS, Bixler HJ. J Polym Sci 1961;50:413–39.
[4] Michaels AS, Vieth WR, Barrie JA. J Appl Phys 1963;34:1–12.
[5] Michaels AS, Vieth WR, Barrie JA. J Appl Phys 1963;34:13–20.
[6] Lowell PN, McCrum NG. J Polym Sci: Part A-2 1971;9:1935–54.
[7] Puleo AC, Paul DR, Wong PK. Polymer 1989;30:1357–66.
[8] Guadagno L, Baldi P, Vittoria V, Guerra G. Macromol Chem Phys 1998;199:2671–5.
[9] Manfredi C, Nobile MAD, Mensitieri G, Guerra G, Rapacciuolo M. J Polym Sci, Part B: Polym Phys 1997;35:133–40.
[10] Budzien JL, McCoy JD, Weinkauf DH, LaViolette RA, Peterson ES. Macromolecules 1998;31:3368–71.
[11] Flory PJ, Yoon DY, Dill KA. Macromolecules 1984;17:862–8.
[12] Kaji H, Horii F. Macromolecules 1997;30:5791–8.
[13] Kitamaru R, Horii F, Murayama K. Macromolecules 1986;19:636–43.
[14] Kitamaru R, Nakaoki T, Alamo RG, Mandelkern L. Macromolecules 1996;29:6847–52.
[15] Mogri Z, Paul DR. Polymer, in press.

[16] Koros WJ, Paul DR, Rocha AA. J Polym Sci: Polym Phys 1976;14:687–702.
[17] Mogri Z, Paul DR. Polymer 2001;42:2531–42.
[18] Chiou JS, Barlow JW, Paul DR. J Appl Polym Sci 1985;30:1173–86.
[19] Michaels AS. AIChE J 1959;5:270–1.
[20] Van Amerongen GJ. J Polym Sci 1947;2:381–6.
[21] Barrer RM, Chio HT. J Polym Sci: Part C 1965;10:111–38.
[22] Van Krevelen DW. Properties of polymers. 3rd ed. New York: Elsevier, 1990.
[23] Paul DR. J Membr Sci 1984;18:75–86.
[24] Koros WJ. J Polym Sci: Polym Phys 1985;23:1611–28.
[25] Raymond PC, Paul DR. J Polym Sci, Part B: Polym Phys 1990;28:2079–102.
[26] Wright CT, Paul DR. Polymer 1997;38:1871–8.
[27] Chiou JS, Paul DR. J Membr Sci 1989;45:167–89.
[28] Van Amerongen GJ. J Polym Sci 1950;5:307–32.
[29] Cowling R, Park GS. J Membr Sci 1979;5:199–207.
[30] Durrill PL, Griskey RG. AIChE J 1966;12:1147–51.
[31] Durrill PL, Griskey RG. AIChE J 1969;15:106–10.